A New Model Reference Self-Tuning Fractional Order PD Control for One Stage Servomechanism System

MOHAMED. A. SHAMSELDIN[1], MOHAMED SALLAM[2], A.M. BASSIUNY[2], & A.M. ABDEL GHANY[3]
[1]Depart. of Mechatronics Eng., Future University in Egypt, Cairo, Egypt,
[2]Department of Mechanical Engineering, Helwan University, Cairo, Egypt
[3]Depart. of Electrical Engineering, October 6 University (Helwan University Originally), Cairo, Egypt
mohamed.abelbbar@fue.edu.eg

Abstract: - This paper presents a new technique to adapt the fractional order PID (FOPID) control based on optimal Model Reference Adaptive System (MRAS). The proposed control technique has been subjected to motion control of one stage servomechanism system. This purpose should be achieved through different operating points and external disorders (friction and backlash). The parameters of MRAS have been obtained using the harmony search (HS) optimization technique to achieve the optimal performance. Also, the performance of proposed control technique has been investigated by comparing it with the PID and FOPID controllers. The practical results illustrate that the self-tuning FOPD control based on optimal model reference adaptive system can accommodate the tracking error rapidly respect to other control techniques.

Key-Words: - Servomechanism; Self-Tuning, Fractional Order PD (FOPD) Control, Model Reference Adaptive System (MRAS), Harmony Research (HS).

1 Introduction

The newest growth of machine tools is to achieve high speed spindle and feed drives which improve the performance and reduce the machining cycle times [1]. Also, the development of feed drives with an adequate dynamic response and smooth behavior has become essential in many industrial applications [2]. The purpose of servo control systems to maintain the stage follows a preselected position profile along complicated trajectories at high feed speeds [3]. The machine tool with traditional feed drives use the proportional position control which suffer from high fluctuation in the stage and large tracking errors at high speeds [4]. The tracking error is eliminated using high performance feed drive motors with advanced control techniques [5]. However, friction between lead screw and guides, cutting force disturbance, and changes in the workpiece mass in linear drives are obstacles to achieve good contouring accuracy at high feeds [6]. The requirements for high speed and accurate contouring have led to the investigation of efficient control algorithms in recent years [7]. The PID control has been used to process control in most of engineering applications for decades [8]. The PID control has simple structure and linear behavior. Also, it gives acceptable performance for several industrial applications [9]. There are several methods to select the proper values for PID controller parameters [3]. The traditional methods for selecting these parameters such as try and error and Ziegler-Nichols which were became inappropriate to achieve a good performance [10]. So, the researchers have tended to use alternative methods such as optimization techniques (Genetic Algorithm (GA), Particle Swarm Optimization (PSO), Ant Colony Optimization (ACO) and Harmony Search (HS)) which are trying to reach the optimal solution for controller parameters [11]. Still, the behavior of PID control is linear and cannot deal with the high disturbance and high nonlinearity of complicated systems [12-13].

The fractional order PID (FOPID) control has been widely used in control engineering in recent decades [14]. The FOPID considers the nonlinear copy of PID control where two more parameters (the fractional integral and derivative) added to the PID control parameters [15]. Hence, the task of designer selecting the proper values for the five parameters of the FOPID control [16]. The FOPID control can solve the nonlinearity problem but it cannot deal with the sudden disturbance due to its parameters which still fixed [17]. A few techniques have been proposed to tune the five parameters of FOPID control online but all of these techniques are based on the fuzzy logic control [18-19]. The fuzzy logic control can solve the uncertainty problem and sudden disturbance but its design depends on the experience which sometimes is not available for some systems [5,20,21]. This study presents a novel

technique to tune the FOPID control parameters online based on optimal model reference adaptive control (MRAC). It is known that the MRAC is high ranking adaptive control where it forces the overall system to follow the behavior of preselected model reference [22]. The preselected model can be first or second order system according to the point of view the designer and complicated degree of the system [23].The task of model reference adaptive control is adjusting the FOPID control parameters online. The model reference contains the desired performance which can satisfy the designer. Moreover, to guarantee high performance the parameters of model reference optimized using the harmony search (HS) optimization technique according to a certain cost function.

The paper has organized as follows, firstly, the experimental setup is presented. Secondly, the proposed control techniques are demonstrated. Thirdly, the simulation results are illustrated. Finally, the conclusion is discussed.

2 Experimental Setup

This section presents the main components of one stage servomechanism system. Also, it shows the open loop performance of servomechanism system through developing accurate identified model for one stage servomechanism system. Fig.1 illustrates the main components of one stage table servomechanism experimental setup which consists of seven parts as the following:

1. One Stage Table: The DC Motor Electro-Mechanical Module demonstrates closed- and open-loop positioning control concepts as well as some electromechanical principles. The stroke of table ranges from 0 to 9 Inch. It consists of a DC motor driving a lead screw on which a sliding block is installed. The DC motor has nominal speed 1800 rev/min, and armature voltage 90 V dc motor.

2. Optical Encoder: An encoder is an electrical mechanical device that can monitor motion or position. A typical encoder uses optical sensors to provide a series of pulses that can be translated into motion. The Optical Encoder is an add-on that provides position feedback signals (100 pulses per revolution).

3. Limit Switches: Two magnetic limit switches detect when the sliding block reaches the start or end position.

4. Motor Driver: The DC Motor Drive controls the DC Motor Electro-Mechanical Module, Model 3293. The drive is configured to operate the motor at one of two user defined speeds. Input signals are used to switch between the two set speeds, to select the direction of motion (forward or reverse), and to enable the movement. This versatile drive also allows an external signal to control the motor speed.

5. A data acquisition card (DAQ) NI USB-6009.

6. Push Buttons, Toggle Switches and Lights: they use to operate the DC motor driver manually.

7. Computer used to perform the control algorithms and receive and send the signals from the NI DAQ Card.

The designed program will make the NI DAQ Card generate random signal ranges from -5V to +5V with sample rate 50 milliseconds which will be input to the DC motor drive. The speed of DC motor will fluctuate with change the generated signal. The positive voltage range of output signal will be made the DC motor speed fluctuates in the forward direction while the DC motor has fluctuated in reverse direction through the negative voltage range. The shaft of the optical encoder will be coupled with lead screw shaft to measure the speed and position of the table. The data will be collected and stored in excel sheet file and then this data will be used to can create identified model for one stage servomechanism system.

The general linear transfer function of such a system may be written as follows:

$$\frac{y(s)}{u(s)} = \frac{k}{b_n.S^n + b_{n-1}.S^{n-1} + \cdots + b_0} \quad (1)$$

Where $y(s)$ is linear speed of one stage table,$u(s)$ is input signal to DC motor driver, n is system order and $k, b_n, \dots, b_0$ are the estimated parameters of the approximate transfer function. It is known that the nonlinear system cannot be represented exactly by linear models. The accuracy of the model can be increased by increasing the order of the linear system. However, often there is a limitation that increasing order cannot improve the model accuracy sufficiently. Therefore, it is necessary to explicitly add the nonlinearities into the system. In this paper, the nonlinear ARX model structure has been applied to model such systems where AR refers to autoregressive part and X to the extra input. The set of candidate identified models have been implemented.

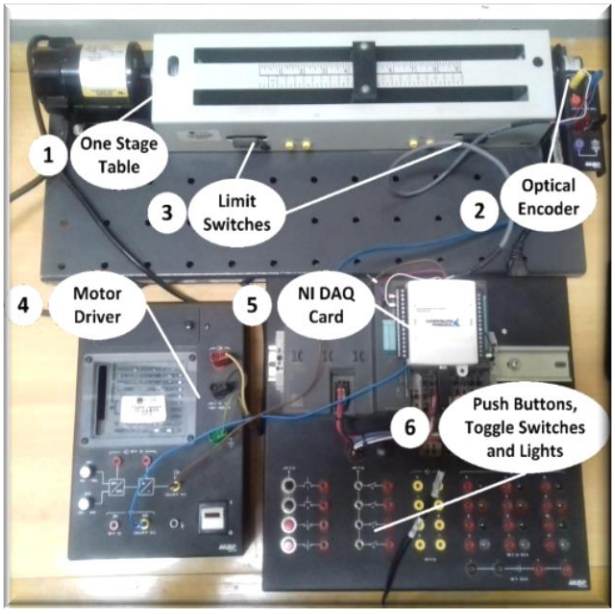

Fig.1 The one Stage Table Servomechanism Experimental Setup

Fig.2 demonstrates the actual experimental setup of one stage table servomechanism and the linear speed of candidate identified models. It is obvious that identified model based on nonlinear least squares can simulate the behavior of actual experimental setup compared to the second order identified model. So, this model will be used to help us to can design and implement advanced control techniques.

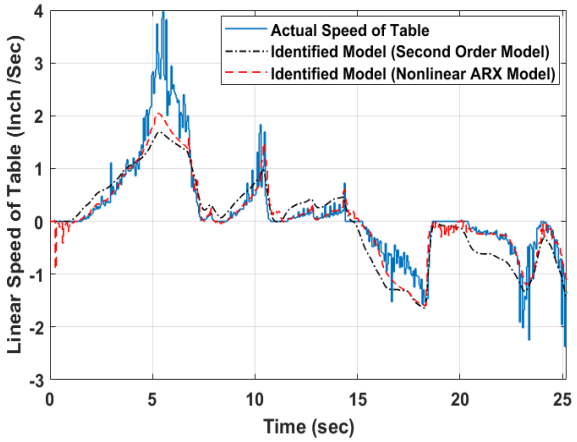

Fig.2 The linear speed of one stage table servomechanism for actual experimental setup and identified models

Table 1 demonstrates the mean square error of each identified model. It can be noted that identified model based on the nonlinear least square method has the minimum error compared to the second order identified model systems.

TABLE 1
MEAN SQUARE ERROR OF CANDIDATES IDENTIFIED MODEL

No.	System Identification Method	Mean Square Error
1	Linear Least Square	0.1973
2	Nonlinear Least Squares	0.05912

3 Control Techniques

This section demonstrates the design steps of three different control techniques. The first technique is the conventional PID control based on Harmony Search (HS). The second technique is the FOPID control based on HS. The third technique is a novel self-tuning FOPID based on optimal model reference adaptive system.

3.1 PID Control

It is well known that the transfer function of the linear PID controller is $K(s) = K_P + K_i/s + K_d s$. Where K_p, K_i and K_d are fixed gains. These gains can be defined as follows. The K_p is the proportional gain which attempt to reduce the error responses. The K_i is the integral gain and its role dampen the steady state error. The K_d is the differential gain which decrease the overshoot of system also, it ensures the system stability [24-25].

In spite of linear fixed parameters PID controllers are often suitable for controlling a simple physical process, the demands for high performance control and systems have different operating points are often beyond the abilities of simple PID controllers [26-27]. In this study, the optimal parameters of PID controller have been obtained using Harmony Search (HS) technique. Harmony search (HS) was suggested by Zong Woo Geem in 2001 [28]. It is well known that HS is a phenomenon-mimicking algorithm inspired by the improvisation process of musicians [29]. The offline optimization has implemented according to the objective function as shown in equation (2) [30].

$$f = \frac{1}{(1-e^{-\beta})(M_p+e_{ss})+e^{-\beta}(t_s-t_r)} \quad (2)$$

Where e_{ss} is the steady state error, M_p is the overshoot of system response, t_s is the settling time and t_r is the rise time. Also, this objective function is able to compromise the designer requirements using the weighting parameter value (β). The

parameter is set larger than 0.7 to reduce over shoot and steady state error. If this parameter is adjusting smaller than 0.7 the rise time and settling time will be reduced. The initial population of Harmony Memory (HM) is chosen randomly.

Fig.3 shows the overall Harmony Search tuning system with PD-PID control. HM consists of Harmony Memory Solution (HMS) vectors. The HM is filled with HMS vectors as follows:

$$HM = \begin{bmatrix} K_{\mathrm{p}\,(1,1)} & K_{\mathrm{i}\,(1,2)} & K_{\mathrm{d}\,(1,3)} & K_{\mathrm{p}\,(1,4)} & K_{\mathrm{d}\,(1,5)} \\ K_{\mathrm{p}\,(2,1)} & K_{\mathrm{i}\,(2,2)} & K_{\mathrm{d}\,(2,3)} & K_{\mathrm{p}\,(2,4)} & K_{\mathrm{d}\,(2,5)} \\ \cdot & \cdot & \cdot & \cdot & \cdot \\ \cdot & \cdot & \cdot & \cdot & \cdot \\ \cdot & \cdot & \cdot & \cdot & \cdot \\ K_{p\,(HMS,1)} & K_{i\,(HMS,2)} & K_{d\,(HMS,3)} & K_{\mathrm{p\,(HMS,4)}} & K_{d\,(HMS,5)} \end{bmatrix} \quad (3)$$

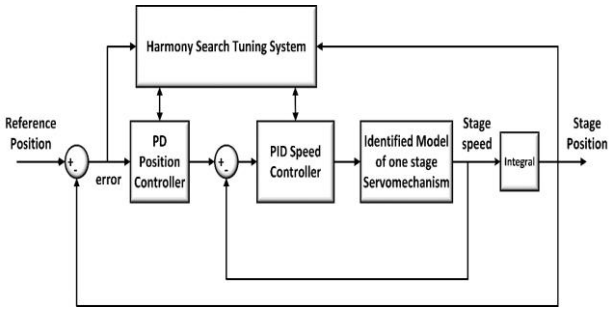

Fig.3 The PD-PID closed loop system with harmony search tuning system

3.2 FOPID Control

The fractional order PID controllers have two more parameters (λ and μ) in addition to the three known parameters of conventional PID controllers proportional (k_p), integral (k_i) and derivative (k_d) parameters. The (λ) and (μ) are the power of (s) in integral and derivative actions respectively. The most common form of a fractional order PID controller is the $PI^{\lambda}D^{\mu}$ where μ and λ can be any real numbers.

The controller transfer function has the form:

$$G_c = \frac{U(s)}{E(s)} = k_p + k_i \frac{1}{s^{\lambda}} + k_d s^{\mu}, (\lambda\,, \mu > 0) \quad (4)$$

The initial population of Harmony Memory (HM) is selected aimlessly. Fig.4 shows the overall Harmony Search tuning system with FOPD-FOPID control [29]. The offline optimization has implemented based on the objective function as shown in equation (2) HM involves Harmony Memory Solution (HMS) vectors. The HM is filled with HMS vectors as follows:

$$HM = \begin{bmatrix} K_{p\,(1,1)} & K_{i\,(1,2)} & K_{d\,(1,3)} & \lambda_{\,(1,4)} & \mu_{\,(1,5)} & K_{p\,(1,6)} & K_{d\,(1,7)} & \mu_{\,(1,8)} \\ K_{p\,(2,1)} & K_{i\,(2,2)} & K_{d\,(2,3)} & \lambda_{\,(2,4)} & \mu_{\,(2,5)} & K_{p\,(2,6)} & K_{d\,(2,7)} & \mu_{\,(2,8)} \\ \cdot & \cdot & \cdot & \cdot & \cdot & \cdot & \cdot & \cdot \\ \cdot & \cdot & \cdot & \cdot & \cdot & \cdot & \cdot & \cdot \\ \cdot & \cdot & \cdot & \cdot & \cdot & \cdot & \cdot & \cdot \\ K_{p\,(HMS,1)} & K_{i\,(HMS,2)} & K_{d\,(HMS,3)} & \lambda_{\,(HMS,4)} & \mu_{\,(HMS,5)} & K_{p\,(HMS,6)} & K_{d\,(HMS,7)} & \mu_{\,(HMS,8)} \end{bmatrix} \quad (5)$$

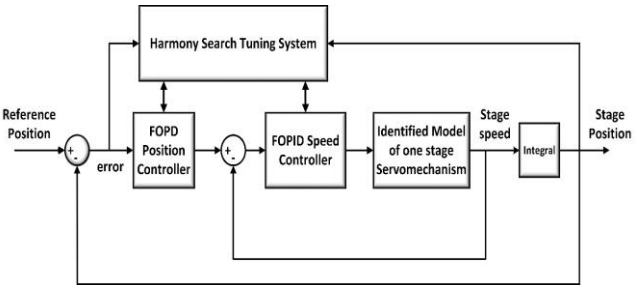

Fig.4 The FOPD-FOPID closed loop system with harmony search tuning system

3.3 Self-Tuning FOPID Control

The Model Reference Adaptive Control (MRAC) is high-ranking adaptive controller [31]. It may be regarded as an adaptive servo system in which the desired performance is expressed in terms of a reference model [22,23,7]. In this work the FOPID control parameters will be adjusted on-line using the model reference technique. Fig.5 presents the structure of self-tuning FOPID based on model reference technique.

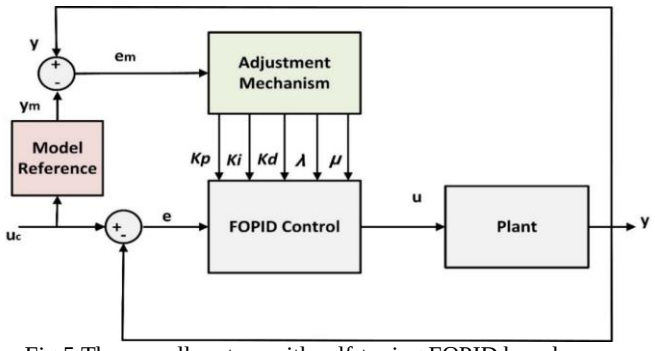

Fig.5 The overall system with self-tuning FOPID based on model reference technique

The MIT rule is the original approach to model reference adaptive control. The name is derived from the fact that it was developed at the Instrumentation Laboratory (now the Draper Laboratory) at MIT. To adjust parameters in such a way that the loss function is minimized.

$$j(\underline{\theta}) = \frac{1}{2} e_m^2 \quad (6)$$

To make j small, it is reasonable to change the parameters in the direction of the negative gradient of j, that is,

$$\frac{d\underline{\theta}}{dt} = -\gamma \frac{\partial j}{\partial \underline{\theta}} = -\gamma e_m \frac{\partial e_m}{\partial \underline{\theta}} \quad (7)$$

Where γ stand for the adaptation gain while $\underline{\theta}$ is the FOPID controller parameters. The transfer function of FOPID control can be described as follows.

$$\frac{u(s)}{e(s)} = k_p + k_i \frac{1}{s^\lambda} + k_d s^\mu \tag{8}$$

$$e = u_c - y \tag{9}$$

Assume that the plant can be simplified to a first order system as obvious in the following equation.

$$\frac{y(s)}{u(s)} = \frac{k}{Ts+1} \tag{10}$$

Where $k \; and \; T$ are unknown parameters. Also, assume that the model reference takes a form first order system as the following relationship.

$$\frac{y_m(s)}{u_c(s)} = \frac{k_m}{T_m s+1} \tag{11}$$

Where $k_m \; and \; T_m$ are selected by designer.

From equations [8-11] can conclude that

$$y = \frac{k}{Ts+1}(k_p + k_i \frac{1}{s^\lambda} + k_d s^\mu)(u_c - y) \tag{12}$$

$$\xrightarrow{yields} \quad y = \frac{kk_p + kk_i \frac{1}{s^\lambda} + kk_d s^\mu}{Ts+1} u_c - \frac{kk_p + kk_i \frac{1}{s^\lambda} + kk_d s^\mu}{Ts+1} y$$

$$\left(1 + \frac{kk_p + kk_i . \frac{1}{s^\lambda} + kk_d s^\mu}{Ts+1}\right) y = \frac{kk_p + kk_i . \frac{1}{s^\lambda} + kk_d s^\mu}{Ts+1} u_c$$

$$\left(\frac{Ts+1+kk_p + kk_i . \frac{1}{s^\lambda} + kk_d s^\mu}{Ts+1}\right) y = \frac{kk_p + kk_i . \frac{1}{s^\lambda} + kk_d s^\mu}{Ts+1} u_c$$

$$y = \frac{kk_p + kk_i . \frac{1}{s^\lambda} + kk_d s^\mu}{Ts+1+kk_p + kk_i . \frac{1}{s^\lambda} + kk_d s^\mu} u_c \tag{13}$$

$$e_m = y - y_m \tag{14}$$

$$e_m = \left[\frac{kk_p + kk_i . \frac{1}{s^\lambda} + kk_d s^\mu}{Ts+1+kk_p + kk_i . \frac{1}{s^\lambda} + kk_d s^\mu} - \frac{k_m}{T_m s+1}\right] u_c \tag{15}$$

3.3.1 Adaptation Law of k_p Parameter

This sub-section shows the steps of design of the adaptation law for proportional gain parameter (k_p). By deriving the equation (15) respect to the proportional gain (k_p) to obtain the following relationship.

$$\frac{\partial e_m}{\partial k_p} = \left[\frac{k}{Ts+kk_p+kk_d s^\mu+kk_i . \frac{1}{s^\lambda}+1} - \frac{k\left(kk_p+kk_i . \frac{1}{s^\lambda}+kk_d s^\mu\right)}{\left(Ts+kk_p+kk_d s^\mu+kk_i . \frac{1}{s^\lambda}+1\right)^2}\right] u_c \tag{16}$$

Equation (16) can be rewritten

$$\frac{\partial e_m}{\partial k_p} = \left[\frac{k\left(Ts+kk_p+kk_i . \frac{1}{s^\lambda}+kk_d s^\mu+1-kk_p-kk_i . \frac{1}{s^\lambda}-kk_d s^\mu\right)}{\left(Ts+kk_p+kk_i . \frac{1}{s^\lambda}+kk_d s^\mu+1\right)^2}\right] u_c \tag{17}$$

$$\frac{\partial e_m}{\partial k_p} = \left[\frac{k(Ts+1)}{\left(Ts+kk_p+kk_i . \frac{1}{s^\lambda}+kk_d s^\mu+1\right)^2}\right] u_c \tag{18}$$

$$\frac{\partial e_m}{\partial k_p} = \left[\frac{k(Ts+1)}{\left(Ts+kk_p+kk_i . \frac{1}{s^\lambda}+kk_d s^\mu+1\right)\left(kk_p+kk_i . \frac{1}{s^\lambda}+kk_d s^\mu\right)}\right] y \tag{19}$$

From equation (17) and equation (19)

$$\frac{\partial e_m}{\partial k_p} = \left[\frac{k^2 e}{\left(Ts+kk_p+kk_i . \frac{1}{s^\lambda}+kk_d s^\mu+1\right)}\right] \tag{20}$$

To achieve the desired performance, the following condition must be hold.

$$Ts + kk_p + kk_i . \frac{1}{s^\lambda} + kk_d s^\mu + 1 = T_m s + 1 \tag{21}$$

$$\frac{\partial e_m}{\partial k_p} = \frac{k^2 e}{T_m s+1} \tag{22}$$

From the MIT rule can obtain the following relationship

$$\frac{dk_p}{dt} = -\gamma . e_m . \frac{k^2 e}{T_m s+1} \tag{23}$$

$$\frac{dk_p}{dt} = -\gamma_1 . \frac{e_m . e}{T_m s+1} \tag{24}$$

$$\gamma_1 = \gamma . k^2 \tag{25}$$

$$k_p)_{new} = \int \frac{dk_p}{dt} \, dt + k_p(0) \tag{26}$$

Where $k_p(0)$ is the initial value of proportional gain k_p.

3.3.2 Adaptation Law of k_i Parameter

This sub-section shows the steps of design of the adaptation law for integral gain parameter (k_i). By deriving the equation (14) respect to the integral gain (k_i) to obtain the following relationship.

$$\frac{\partial e_m}{\partial k_i} = \frac{1}{s^\lambda}\left[\frac{k}{Ts+kk_p+kk_d s^\mu+kk_i.\frac{1}{s^\lambda}+1} - \frac{k\left(kk_p+kk_i.\frac{1}{s^\lambda}+kk_d s^\mu\right)}{\left(Ts+kk_p+kk_d s^\mu+kk_i.\frac{1}{s^\lambda}+1\right)^2}\right]u_c \tag{27}$$

Equation (27) can be rewritten

$$\frac{\partial e_m}{\partial k_i} = \frac{1}{s^\lambda}\left[\frac{k\left(Ts+kk_p+kk_i.\frac{1}{s^\lambda}+kk_d s^\mu+1-kk_p-kk_i.\frac{1}{s^\lambda}-kk_d s^\mu\right)}{\left(Ts+kk_p+kk_i.\frac{1}{s^\lambda}+kk_d s^\mu+1\right)^2}\right]u_c \tag{28}$$

$$\frac{\partial e_m}{\partial k_i} = \frac{1}{s^\lambda}\left[\frac{k(Ts+1)}{\left(Ts+kk_p+kk_i.\frac{1}{s^\lambda}+kk_d s^\mu+1\right)^2}\right]u_c \tag{29}$$

$$\frac{\partial e_m}{\partial k_i} = \frac{1}{s^\lambda}\left[\frac{k(Ts+1)}{\left(Ts+kk_p+kk_i.\frac{1}{s^\lambda}+kk_d s^\mu+1\right)\left(kk_p+kk_i.\frac{1}{s^\lambda}+kk_d s^\mu\right)}\right]y \tag{30}$$

From equation (28) and equation (30)

$$\frac{\partial e_m}{\partial k_i} = \frac{1}{s^\lambda}\left[\frac{k^2 e}{\left(Ts+kk_p+kk_i.\frac{1}{s^\lambda}+kk_d s^\mu+1\right)}\right] \tag{31}$$

To achieve the desired performance, the condition must be hold in equation (15).

$$\frac{\partial e_m}{\partial k_i} = \frac{1}{s^\lambda}\frac{k^2 e}{T_m s+1} \tag{32}$$

From the MIT rule can obtain the following relationship

$$\frac{dk_i}{dt} = -\gamma.e_m.\frac{1}{s^\lambda}\frac{k^2 e}{T_m s+1} \tag{33}$$

$$\frac{dk_i}{dt} = -\gamma_2.\frac{e_m.e}{T_m s+1} \tag{34}$$

$$\gamma_2 = \gamma k^2.\frac{1}{s^{\lambda(0)}} = \gamma_1\frac{1}{s^{\lambda(0)}} \tag{35}$$

$$k_i)_{new} = \int \frac{dk_i}{dt}\,dt + k_i(0) \tag{36}$$

Where $k_i(0)$ is the initial value of proportional gain k_i.

3.3.3 Adaptation Law of k_d Parameter

This sub-section illustrates the steps of design of the adaptation law for derivative gain parameter (k_d). By deriving the equation (15) respect to the derivative gain (k_d) to obtain the following relationship.

$$\frac{\partial e_m}{\partial k_d} = \left[\frac{ks^\mu}{Ts+kk_p+kk_i\frac{1}{s^\lambda}+kk_d s^\mu+1} - \frac{ks^\mu\left(kk_p+kk_i\frac{1}{s^\lambda}+kk_d s^\mu\right)}{\left(Ts+kk_p+kk_i\frac{1}{s^\lambda}+kk_d s^\mu+1\right)^2}\right]u_c \tag{37}$$

$$\frac{\partial e_m}{\partial k_d} = \left[\frac{ks^\mu\left(Ts+kk_p+kk_i\frac{1}{s^\lambda}+kk_d s^\mu+1-kk_p-kk_i\frac{1}{s^\lambda}-kk_d s^\mu\right)}{\left(Ts+kk_p+kk_i\frac{1}{s^\lambda}+kk_d s^\mu+1\right)^2}\right]u_c \tag{38}$$

$$\frac{\partial e_m}{\partial k_d} = \left[\frac{ks^\mu(Ts+1)}{\left(Ts+kk_p+kk_i\frac{1}{s^\lambda}+kk_d s^\mu+1\right)^2}\right]u_c \tag{39}$$

$$\frac{\partial e_m}{\partial k_d} = \left[\frac{ks^\mu(Ts+1)}{\left(Ts+kk_p+kk_i\frac{1}{s^\lambda}+kk_d s^\mu+1\right)\left(kk_p+kk_i\frac{1}{s^\lambda}+kk_d s^\mu\right)}\right]y \tag{40}$$

Also, from equation (38) and equation (40)

$$\frac{\partial e_m}{\partial k_d} = \left[\frac{k^2.s^\mu.e}{\left(Ts+kk_p+kk_i\frac{1}{s^\lambda}+kk_d s^\mu+1\right)}\right] \tag{41}$$

$$\frac{\partial e_m}{\partial k_d} = \frac{k^2.s^\mu.e}{T_m s+1} \tag{42}$$

$$\frac{dk_d}{dt} = -\gamma.e_m.\frac{k^2.s^\mu.e}{T_m s+1} \tag{43}$$

$$\frac{dk_d}{dt} = -\gamma_3.\frac{e_m.e}{T_m s+1} \tag{44}$$

$$\gamma_3 = \gamma.k^2.s^{\mu(0)} = \gamma_1.s^{\mu(0)} \tag{45}$$

$$k_d)_{new} = \int \frac{dk_d}{dt}\,dt + k_d(0) \tag{46}$$

Where $k_d(0)$ is the initial value of derivative gain k_d.

3.3.4 Adaptation Law of λ Parameter

This sub-section illustrates the steps of design of the adaptation law for fractional integral gain parameter (λ). By deriving the equation (15) respect to the fractional integral gain (λ) to obtain the following relationship.

$$\frac{\partial e_m}{\partial \lambda} = \frac{kk_i ln(s)}{s^{\lambda}}\left[\frac{\left(kk_p+kk_i\frac{1}{s^{\lambda}}+kk_d s^{\mu}\right)}{\left(Ts+kk_p+kk_i\frac{1}{s^{\lambda}}+kk_d s^{\mu}+1\right)^2} - \frac{1}{(Ts+kk_p+kk_i\frac{1}{s^{\lambda}}+kk_d s^{\mu}+1)}\right]u_c \quad (47)$$

$$\frac{\partial e_m}{\partial \lambda} = \frac{kk_i ln(s)}{s^{\lambda}}\left[\frac{kk_p+kk_i\frac{1}{s^{\lambda}}+kk_d s^{\mu}-Ts-kk_p-kk_i\frac{1}{s^{\lambda}}-kk_d s^{\mu}-1}{\left(Ts+kk_p+kk_i\frac{1}{s^{\lambda}}+kk_d s^{\mu}+1\right)^2}\right]u_c \quad (48)$$

$$\frac{\partial e_m}{\partial \lambda} = \frac{kk_i ln(s)}{s^{\lambda}}\left[\frac{-(Ts+1)}{\left(Ts+kk_p+kk_i\frac{1}{s^{\lambda}}+kk_d s^{\mu}+1\right)^2}\right]u_c \quad (49)$$

$$\frac{\partial e_m}{\partial \lambda} = \frac{kk_i ln(s)}{s^{\lambda}}\left[\frac{-(Ts+1)}{\left(Ts+kk_p+kk_i\frac{1}{s^{\lambda}}+kk_d s^{\mu}+1\right)\left(kk_p+kk_i\frac{1}{s^{\lambda}}+kk_d s^{\mu}\right)}\right]y \quad (50)$$

Also, from equation (48) and equation (50)

$$\frac{\partial e_m}{\partial \lambda} = -\frac{k^2 k_i ln(s)}{s^{\lambda}}\left[\frac{e}{\left(Ts+kk_p+kk_i\frac{1}{s^{\lambda}}+kk_d s^{\mu}+1\right)}\right] \quad (51)$$

$$\frac{\partial e_m}{\partial \lambda} = -\frac{k^2 k_i ln(s)}{s^{\lambda}}.\frac{e}{T_m s+1} \quad (52)$$

$$\frac{d\lambda}{dt} = \gamma.e_m.\frac{k^2 k_i ln(s)}{s^{\lambda}}.\frac{e}{T_m s+1} \quad (53)$$

$$\frac{d\lambda}{dt} = \gamma_4.\frac{e_m.e}{T_m s+1} \quad (54)$$

$$\gamma_4 = \gamma.\frac{k^2 k_i(0)\, ln(s)}{s^{\lambda(0)}} = \gamma_2.k_i(0).ln(s) \quad (55)$$

$$\lambda)_{new} = \int \frac{d\lambda}{dt}\, dt + \lambda(0) \quad (56)$$

Where $\lambda(0)$ is the initial value of fractional integral gain λ.

3.3.5 Adaptation Law of μ Parameter

This sub-section demonstrates the steps of design of the adaptation law for fractional derivative gain parameter (μ). By deriving the equation (15) respect to the fractional derivative gain (μ) to obtain the following relationship.

$$\frac{\partial e_m}{\partial \mu} = \left[\frac{kk_d.s^{\mu}.ln(s)}{Ts+kk_p+kk_i\frac{1}{s^{\lambda}}+kk_d s^{\mu}+1} - \frac{kk_d.s^{\mu}.ln(s)\left(kk_p+kk_i\frac{1}{s^{\lambda}}+kk_d s^{\mu}\right)}{\left(Ts+kk_p+kk_i\frac{1}{s^{\lambda}}+kk_d s^{\mu}+1\right)^2}\right]u_c \quad (57)$$

$$\frac{\partial e_m}{\partial \mu} = \left[\frac{kk_d.s^{\mu}.ln(s)\left(Ts+kk_p+kk_i\frac{1}{s^{\lambda}}+kk_d s^{\mu}+1-kk_p-kk_i\frac{1}{s^{\lambda}}-kk_d s^{\mu}\right)}{\left(Ts+kk_p+kk_i\frac{1}{s^{\lambda}}+kk_d s^{\mu}+1\right)^2}\right]u_c \quad (58)$$

$$\frac{\partial e_m}{\partial \mu} = \left[\frac{kk_d.s^{\mu}.ln(s)(Ts+1)}{\left(Ts+kk_p+kk_i\frac{1}{s^{\lambda}}+kk_d s^{\mu}+1\right)^2}\right]u_c \quad (59)$$

$$\frac{\partial e_m}{\partial \mu} = \left[\frac{kk_d.s^{\mu}.ln(s)(Ts+1)}{\left(Ts+kk_p+kk_i\frac{1}{s^{\lambda}}+kk_d s^{\mu}+1\right)\left(kk_p+kk_i\frac{1}{s^{\lambda}}+kk_d s^{\mu}\right)}\right]y \quad (60)$$

Also, from equation (58) and equation (60)

$$\frac{\partial e_m}{\partial \mu} = \left[\frac{k^2 k_d.s^{\mu}.ln(s).e}{\left(Ts+kk_p+kk_i\frac{1}{s^{\lambda}}+kk_d s^{\mu}+1\right)}\right] \quad (61)$$

$$\frac{\partial e_m}{\partial \mu} = \frac{k^2 k_d.s^{\mu}.ln(s).e}{T_m s+1} \quad (62)$$

$$\frac{d\mu}{dt} = -\gamma.e_m.\frac{k^2 k_d.s^{\mu}.ln(s).e}{T_m s+1} \quad (63)$$

$$\frac{d\mu}{dt} = -\gamma_5.\frac{e_m.e}{T_m s+1} \quad (64)$$

$$\gamma_5 = \gamma.k^2.k_d(0).s^{\mu(0)}.ln(s) = \gamma_3.k_d(0).ln(s) \quad (65)$$

$$\mu)_{new} = \int \frac{d\mu}{dt}\, dt + \mu(0) \quad (66)$$

Where $\mu(0)$ is the initial value of fractional integral gain μ.

The adaptation gains can be obtained using the Harmony Search (HS) optimization based on the objective function in equation (2). The initial population of Harmony Memory (HM) is produced randomly. HM contains Harmony Memory Solution (HMS) vectors. The HM is filled with HMS vectors as follows:

$$HM = \begin{bmatrix} \gamma_{1\,(1,1)} & \gamma_{2(1,2)} & \gamma_{3\,(1,3)} & \gamma_{4\,(1,4)} & \gamma_{5(1,5)} \\ \gamma_{1\,(2,1)} & \gamma_{2(2,2)} & \gamma_{3(2,3)} & \gamma_{4\,(2,4)} & \gamma_{5(2,5)} \\ . & . & . & . & . \\ . & . & . & . & . \\ . & . & . & . & . \\ \gamma_{1\,(HMS,1)} & \gamma_{2\,(HMS,2)} & \gamma_{3(HMS,3)} & \gamma_{4\,(\mathrm{HMS},4)} & \gamma_{5(HMS,5)} \end{bmatrix} \quad (67)$$

The self-tuning FOPID control will be applied as position control in one stage servomechanism system. So, the integral part will be eliminated to become self-tuning FOPD control as shown in Fig.6.

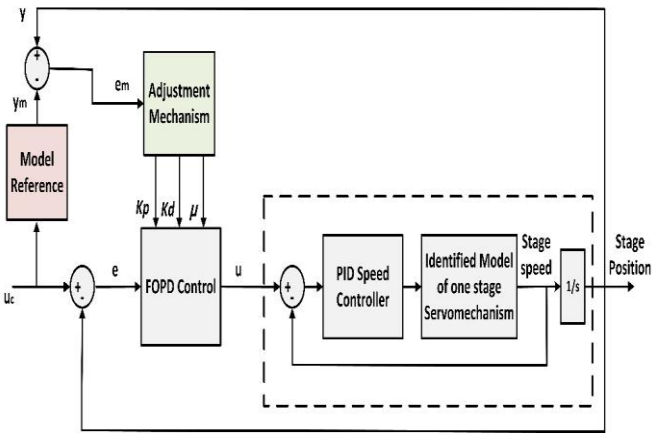

Fig.6 The overall system with self-tuning FOPID based on model reference technique

4 Experimental Results

This section demonstrates the experimental results of different control techniques which has mentioned in the previous section. There are two tests will be implemented to investigate each control technique. The first test is applied at constant position reference while the second test is subjected at variable position reference.

4.1 Constant position reference

This test considers the position reference at constant value (7 inch) and the stage has adjusted at zero inch. Fig.7 illustrates the responses of stage position using three different control techniques. It can be noted that the self-tuning FOPD-PID control has minimum rise time and more smoothly behavior compared to other control techniques. Also, the self-tuning FOPD-PID control has a very small overshoot in a small time.

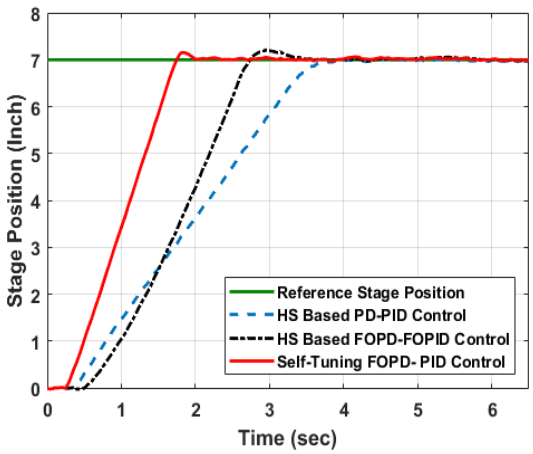

Fig.7 The actual stage position response of each control technique at constant position reference

Fig.8 demonstrates the corresponding stage speed responses through the experiment. It can be obvious that the self-tuning FOPID-PID control has high speed at the rise time period. Also, it has undershoot in speed at moment 2 second to can compensate the overshoot in stage position. Then, the stage speed stables at zero approximately.

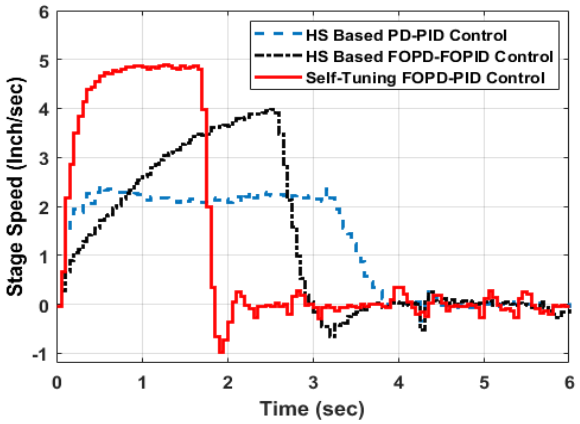

Fig.8 The corresponding stage speed response of each control technique at constant position reference.

Fig.9 displays the corresponding position controllers output through the experiment. It is clear that controller's outputs have maximum value at rise time period and then they reduce suddenly to zero when the stage reach the required position.

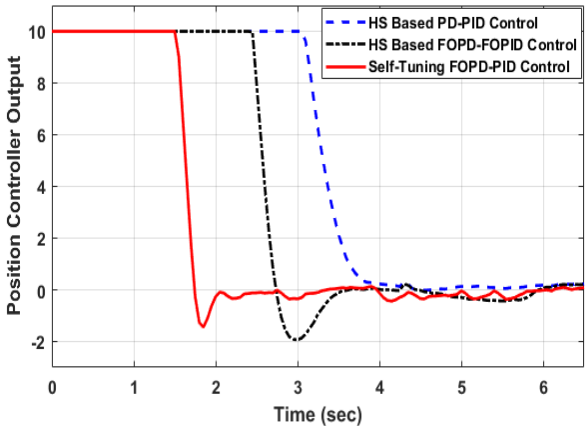

Fig.9 The position controller output response of each control technique at constant position reference

Fig.10 demonstrates the corresponding speed controllers output through the experiment. The speed controller output of self-tuning FOPD-PID control has a maximum value compared to other control techniques which makes the stage accelerated rapidly to reach the position reference.

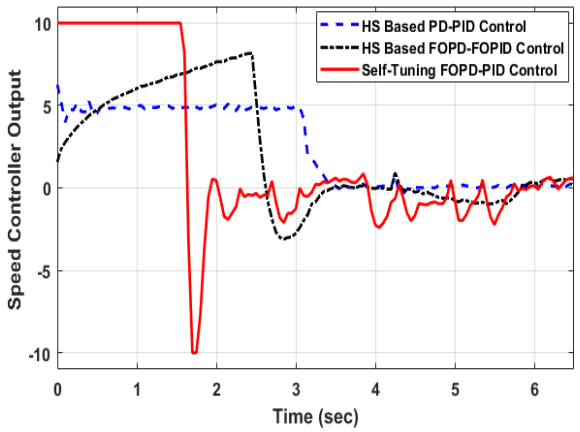

Fig.10 The speed controller output response of each control technique at constant position reference

4.2 Variable Position Reference

The position reference in this test changes continuously to measure the control performance and its ability to track different types of position reference trajectories. Figure 11 shows the stage position behaviors using several control techniques and at variable position reference. It can be noted that the self-tuning FOPD-FOPID control can track accurately the complicated trajectory respect to other control techniques. Also, the HS Based FOPD-FOPID control has acceptable tracking accuracy but it has a high error in the beginning of tracking while the HS Based PD-PID control has a high deviation about the position reference trajectory.

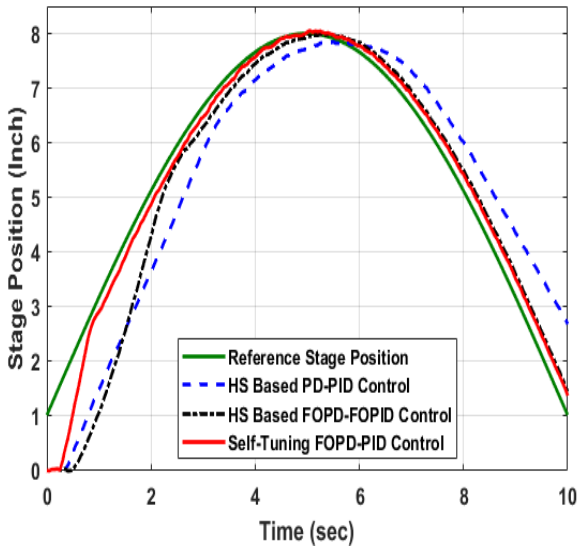

Fig.11 The actual stage position response of each control technique at variable position reference

Fig.12 demonstrates the corresponding stage speed responses for each control technique. It can be noted that the stage speed of self-tuning FOPD-FOPID control is very high through the first seconds of experiment and then the stage speed decreases gradually to can to can track the position reference trajectory.

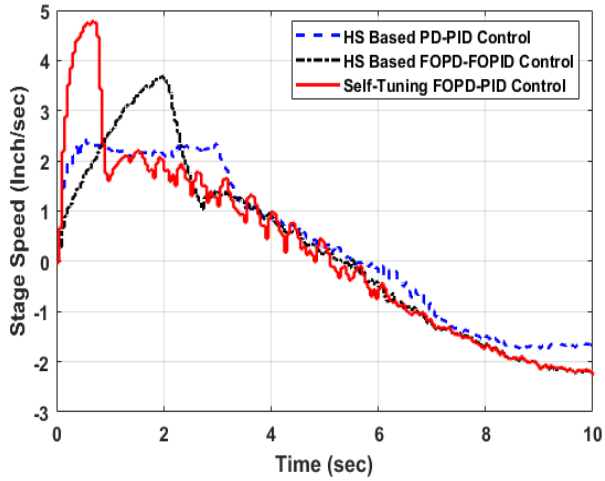

Fig.12 The corresponding speed stage response of each control technique at variable position reference

Fig.13 shows the corresponding position controllers output through the variable position reference experiment. It is clear that in the first seconds of experiments the controllers output has a high value and then the controller's outputs decrease gradually but at different times for each control technique until the signals polarity change to can the stage reverses its direction.

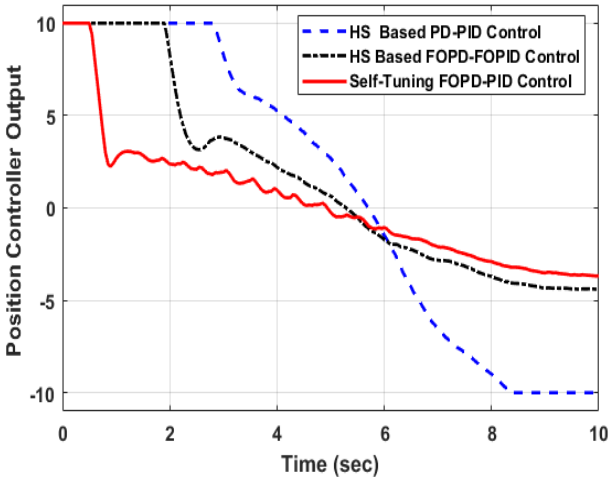

Fig.13 The position controller output response of each control technique at variable position reference.

Fig.14 demonstrates the corresponding speed controllers output for each control technique through the variable position reference experiment. It can be noted that the speed control signal of self-tuning FOPD-FOPID control reach the maximum value in the first seconds of experiment respect to other control techniques. Then, the value of each control technique reduces gradually until the polarity of signals change to can the direction of stage reverses automatically.

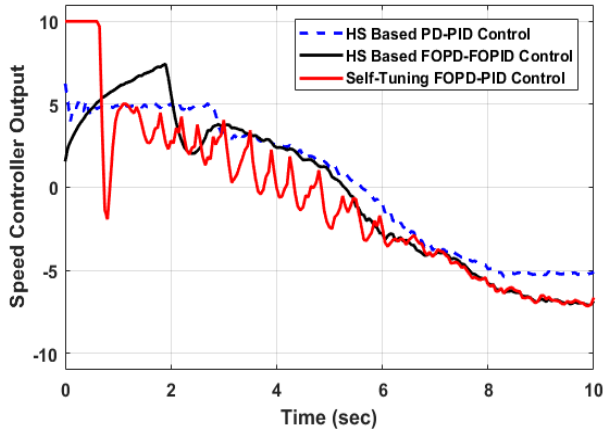

Fig.14 The speed controller output response of each control technique at variable position reference.

4 Conclusion

A new technique has been developed to tune the fractional order PID (FOPID) control online based on optimal Model Reference Adaptive Control (MRAC). This work investigates the robustness of the proposed technique by applied it on one stage servomechanism system. The purpose of controller to track accurately a preselected position reference trajectory although the friction and backlash problems. Also, the performance of the proposed control technique has been compared to the PID and the FOPID control to ensure the robustness. There are two tests have been implemented to investigate each control technique. The first test adjusts the position reference at constant value while the second test tunes the position reference to change continuously with time. The experimental results demonstrate that the self-tuning FOPD control based on optimal model reference adaptive system can eliminate the tracking error quickly compared to other control techniques.

References:

[1] E. Yuliza, H. Habil, R. A. Salam, M. M. Munir, and M. Abdullah, "Development of a Simple Single-Axis Motion Table System for Testing Tilt Sensors," Procedia Eng., vol. 170, pp. 378–383, 2017.

[2] P. Zhao, J. Huang, and Y. Shi, "Nonlinear dynamics of the milling head drive mechanism in five-axis CNC machine tools," Int. J. Adv. Manuf. Technol., 2017.

[3] P. Perz, I. Malujda, D. Wilczy, and P. Tarkowski, "Methods of controlling a hybrid positioning system using LabVIEW," Procedia Eng., vol. 177, pp. 339–346, 2017.

[4] F. L. Li, M. L. Mi, and Y. Z. N. Jin, "Friction identification and compensation design for precision positioning," Springer, pp. 120–129, 2017.

[5] M. Irfan, M. Effendy, N. Alif, S. Lailis, I. Pakaya, and A. Faruq, "Performance Comparison of Fuzzy Logic and Proportional-integral for an Electronic Load Controller," Int. J. Power Electron. Drive Syst., vol. 8, no. 3, pp. 1176–1183, 2017.

[6] A. Franchi and A. Mallet, "Adaptive Closed-loop Speed Control of BLDC Motors with Applications to Multi-rotor Aerial Vehicles," in 2017 IEEE International Conference on Robotics and Automation (ICRA) Singapore., 2017, no. 978, pp. 5203–5208.

[7] S. Wen, T. Wang, Z. Ma, and X. Li, "Dynamics Modeling and Fuzzy PD Control of Humanoid Arm," in Proceedings of the 36th Chinese Control Conference, 2017, no. 3, pp. 616–621.

[8] A. Scientiarum, "dSPACE real time implementation of fuzzy PID position controller for vertical rotating single link arm robot using four-quadrant BLDC drive," pp. 301–311, 2017.

[9] R. Madiouni, "Robust PID Controller Design based on Multi-Objective Particle Swarm Optimization Approach," in ICEMIS2017, 2017, pp. 1–7.

[10] B. Zhang, G. Cheng, and J. Hu, "An Expanded Proximate Time-optimal Servo Controller Design for Fast Set-point Motion," Proc. 35th Chinese Control Conf. July, no. 2, pp. 4465–4470, 2016.

[11] M. Omar, M. A. Ebrahim, A. M, and F. Bendary, "Tuning of PID Controller for Load Frequency Control Problem via Harmony Search Algorithm," Indones. J. Electr. Eng. Comput. Sci., vol. 1, no. 2, pp. 255–263, 2016.

[12] D. Vanitha and M. Rathinakumar, "Fractional Order PID Controlled PV Buck Boost Converter with Coupled Inductor,"

Int. J. Power Electron. Drive Syst., vol. 8, no. 3, pp. 1401–1407, 2017.

[13] M. A. A. Ghany, M. A. Shamseldin, and A. M. A. Ghany, "A Novel Fuzzy Self Tuning Technique of Single Neuron PID Controller for Brushless DC Motor," Int. J. Power Electron. Drive Syst., vol. 8, no. 4, pp. 1705–1713, 2017.

[14] M. A. Shamseldin, A. A. El-samahy, and A. M. A. Ghany, "Different Techniques of Self-Tuning FOPID Control for Brushless DC Motor," in MEPCON, 2016.

[15] P. Kumar and S. Narayan, "Optimal design of robust FOPID for the aircraft pitch control system using multi-objective GA," 2016 IEEE Students' Conf. Electr. Electron. Comput. Sci., pp. 1–6, 2016.

[16] D. Tiwari, N. Pachauri, A. Rani, and V. Singh, "Fractional order PID (FOPID) controller based temperature control of bioreactor," Int. Conf. Electr. Electron. Optim. Tech. ICEEOT 2016, pp. 2968–2973, 2016.

[17] M. A. K. El-shafei, M. I. El-hawwary, and H. M. Emara, "Implementation of Fractional - Order PID Controller in an Industrial Distributed Control System," in 2017 14th International Multi-Conference on Systems, Signals & Devices (SSD) Implementation, 2017, no. 3, pp. 713–718.

[18] I. Masngut et al., "Design of Fractional-Order Proportional-Integral-Derivative Controller : Hardware Realization," in 2018 International Conference on Information and Communications Technology (ICOIACT) Design, 2018, no. 3, pp. 656–660.

[19] M. A. Shamseldin and A. A. El-samahy, "Speed Control of BLDC Motor By Using PID Control and Self-tuning Fuzzy PID controller," 2014.

[20] X. Gao, W. Zhao, and J. Huang, "On-line Parameter Identification and Control Parameters Optimization of Robot Joints with Unknown Load Torque," no. Icsai, pp. 61–66, 2016.

[21] D. V. L. N. Sastry and M. S. R. Naidu, "An Implementation of Different Non Linear PID Controllers on a Single Tank level Control using Matlab," Int. J. Comput. Appl., vol. 54, no. 1, pp. 6–8, 2012.

[22] S. Slama, A. Errachdi, M. Benrejeb, A. R. B. F. Neural, and N. Identification, "Model Reference Adaptive Control for MIMO Nonlinear Systems Using RBF Neural Networks," in 2018 International Conference on Advanced Systems and Electric Technologies (IC_ASET), 2018, pp. 346–351.

[23] L. Zhu, X. Shi, Z. Chen, H. Zhang, and C. Xiong, "Adaptive Servomechanism of Pneumatic Muscle Actuators With Uncertainties," IEEE Trans. Ind. Electron., vol. 64, no. 4, pp. 3329–3337, 2017.

[24] L. Abdullah et al., "Evaluation on Tracking Performance of PID , Gain Scheduling and Classical Cascade P / PI Controller on XY Table Ballscrew Drive System Faculty of Manufacturing Engineering , Universiti Teknikal Malaysia Melaka (UteM)," vol. 21, pp. 1–10, 2013.

[25] T. Nadu and P. Magnet, "Modeling and Implementation of Intelligent Commutation System for BLDC Motor in Underwater Robotic Applications," in 1st IEEE International Conference on Power Electronics. Intelligent Control and Energy Systems (ICPEICES-2016) Modeling, 2016, pp. 1–4.

[26] Y. X. Su, D. Sun, and B. Y. Duan, "Design of an enhanced nonlinear PID controller," Mechatronics, vol. 15, pp. 1005–1024, 2005.

[27] S. B. U, "Multivariable Centralized Fractional Order PID Controller tuned using Harmony search Algorithm for Two Interacting Conical Tank Process," in SAI Intelligent Systems Conference 2015 November 10-11, 2015 | London, UK Multivariable, 2015, pp. 320–327.

[28] M. Omar, A. M. A. Ghany, and F. Bendary, "Harmony Search based PID for Multi Area Load Frequency Control Including Boiler Dynamics and Nonlinearities," WSEAS Trans. CIRCUITS Syst., vol. 14, pp. 407–414, 2015.

[29] M. A. Ebrahim and F. Bendary, "Reduced Size Harmony Search Algorithm for Optimization," J. Electr. Eng., pp. 1–8, 2016.

[30] A. A. El-samahy and M. A. Shamseldin, "Brushless DC motor tracking control using self-tuning fuzzy PID control and model reference adaptive control," Ain Shams Eng. J., 2016.

[31] K. Hossain and S. M. R. Islam, "Model Reference Adaptive Control for Surface Permanent Magnet Synchronous Machine," no. December, pp. 7–9, 2017.